Nuclear Physics B85 (1975) 141–157. North-Holland Publishing Company

SCALING IN pp ELASTIC SCATTERING

P.D.B. COLLINS, F.D. GAULT and A. MARTIN
Physics Department, University of Durham, Durham City, England

Received 30 September 1974

Abstract: Various scaling laws such as $d\sigma/dt \sim s^{-n} f(z)$ are tested against the large $|t|$ pp elastic scattering data including that from ISR. We draw the following tentative conclusions. (a) The ISR data are not incompatible with scaling for $|t| > 2.4$ GeV^2. (b) This scaling seems to be a property of the P ⊗ P cut not the P (pomeron) pole. (c) But the power n seems to decrease from about 11.5 at $z = 0$ to 9 or less at $z = 0.99$ (at large s) which could be due to the Landshoff diagram or eikonalisation becoming important, making scaling just a low energy phenomenon. (d) Though $f(z)$ has a fairly simple structure it does not seem to be directly related to the proton's electromagnetic form factor.

1. Introduction

The somewhat paradoxical success of the free quark-parton model in describing the scaling behaviour of deep inelastic scattering of leptons and hadrons [1] has led several authors to try and extend these ideas to large momentum transfer inclusive and exclusive hadron scattering processes. (For reviews see refs. [2, 3]). Various scaling laws have been postulated, but the identification of the most important diagrams depends on the assumptions which are made about the couplings of quarks to hadrons, and the nature of the quark-quark scattering amplitude, and different authors have been led to somewhat different scaling rules.

Our purpose in this paper is to try and evaluate the phenomenological success of these various suggestions by comparing them with the data on the pp elastic scattering, which, thanks to recent work at the CERN-ISR, is now available over a large range of s, and a reasonable t range.

The plan of the paper is as follows. In sect. 2 we briefly review the principal models which are in contention, and the attempts which have been made to verify them. In sect. 3 we discuss the data set, and the method used to interpolate between low and high s. This is followed by discussions of the s dependence at fixed z ($z \equiv$ the cosine of the c.m. scattering angle), the z dependence at fixed s, and of some fits using models which are based on the assumption that information about the quark-hadron couplings may be obtained from the behaviour of the electromagnetic form factors of the hadrons. Some conclusions are presented in sect. 7.

2. Models of scaling in exclusive processes

In 1968 Abarbanel *et al.* [4] proposed (following a suggestion of Yang and collaborators [5, 6] concerning the small $|t|$ behaviour) that at large $|t|$ hadronic elastic scattering was dominated by quark-quark (q-q) scattering, as shown in fig. 1a. The q-q amplitude was supposed to be a point-like vector gluon interaction independent of s and t, while the quark-hadron (q-H) couplings could be determined from the electromagnetic form factors of the hadrons which were supposed to be given by fig. 1b. This gave (for AB → AB)

$$\frac{d\sigma}{dt} \propto [G_A(t)\, G_B(t)]^2, \tag{2.1}$$

where the G's are the form factors. Thus for pp → pp, if $G_p(t) \sim (t)^{-2}$ they predict

$$\frac{d\sigma}{dt}\,(pp) \sim \frac{1}{t^8}\ , \tag{2.2}$$

at fixed s. This is not in accord with the low-energy data, however, and instead Horn and Moshe [7] proposed that the q–q scattering amplitude should be a scaling function of z only,

$$z = 1 + \frac{2t}{s-4m^2} \approx 1 + \frac{2t}{s} \approx -1 - \frac{2u}{s}\,, \tag{2.3}$$

(m = nucleon mass), but need not be a constant as above, and so they postulated

$$\frac{d\sigma}{dt} \propto [G_A(t)\, G_B(t)]^2\, f(z). \tag{2.4}$$

So at fixed z they obtain

$$\frac{d\sigma}{dt}\,(pp) \approx \frac{1}{s^n}\, f(z), \tag{2.5}$$

with $n \simeq 8$. Note that possible log s factors from the loop integrations have been neglected in obtaining this result. For the z dependence they used various exponential forms such as

$$f(z) = A e^{-at/s}, \tag{2.6}$$

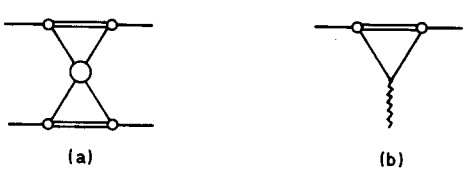

Fig. 1(a) Proton-proton scattering proceeding via q–q scattering. (b) Quark model for the electromagnetic form factor.

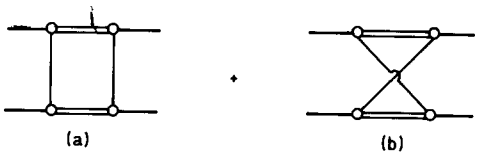

Fig. 2. Quark interachange diagrams for pp scattering. The double line across the middle of the diagram represents the proton "core" left when a quark has been emitted.

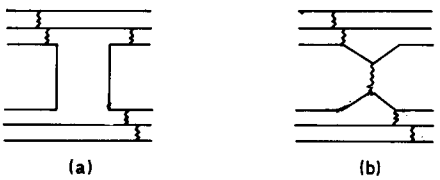

Fig. 3. Quark interchange (a) and scattering (b) diagrams used to predict scaling behaviour in pp scattering in ref. [13].

and claimed quite a good fit to the $s < 50$ GeV^2 pp data with $n = 9.3$.

Alternatively Gunion *et al.* [8,9] supposed that at large t the dominant mechanism would be the exchange of the constituent quarks between the protons, as in fig. 2. Assuming that the electromagnetic form factor is given by fig. 1b they obtained

$$\frac{d\sigma}{dt} \propto [G_p(s)\, G_p(t)\, G_p(u)]^2 I(z) \to \frac{1}{s^{12}} \frac{1}{(1-z^2)^4} I(z) \tag{2.8}$$

at fixed z, if $G_p(t) \sim t^{-2}$. This is also claimed [9] to fit the low energy data with $I(z) \propto (1-z^2)^{-1.2}$.

Landshoff and Polkinghorne [10] supported Gunion *et al.* in supposing that fig. 2 is more important than fig. 1a at large $|t|$ because they expect that q–H scattering $\to 0$ as the virtual quark mass $(m_q) \to \infty$, but they suggested that without further assumptions which are hard to justify all that one should read from fig. 2 is the general form

$$\frac{d\sigma}{dt} \sim \frac{1}{s^n} f(z) \tag{2.9}$$

(neglecting log s terms), and from a fit to the data [11] they found $n = 9.7 \pm 0.5$, $f(z) \propto (1-z^2)^{-7}$ for $|t| > 2.5$ GeV^2, $s > 15$ GeV^2. Similarly Barger *et al.* [12], found that $n = 9.3$ for $0.4 > z > 0$, but at higher energies $n \approx 10$ was needed.

This accords with the proposal of Brodsky and Farrar [13] that if the quarks have a scale invariant interaction (independent of s) then both the interchange (fig. 3a) and q-q scattering (fig. 3b) diagrams give the behaviour

$$\frac{d\sigma}{dt} \sim s^{2-\Sigma} f(z), \tag{2.10}$$

where Σ is the total number of quarks entering and leaving the diagram. Thus for

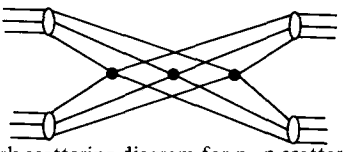

Fig. 4. Wide angle triple quark scattering diagram for p–p scattering considered in ref. [14].

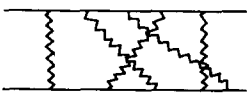

Fig. 5. An example of a multiple exchange eikonal diagram.

qq → qq $\Sigma = 4$, giving the scale invariant behaviour $d\sigma/dt \sim s^{-2}$, while for pp elastic scattering $\Sigma = 12$ giving the scaling rule

$$\frac{d\sigma}{dt} \sim s^{-10} f(z). \tag{2.11}$$

This differs from (2.8) because Gunion *et al.* [8, 9] treat the proton as an essentially two-component object (quark + core in fig. 2) rather than the 3q form used in fig. 3. The power law (2.10) seems to work well also for the low energy data on meson-baryon and photon-baryon scattering [2, 3].

However, Landshoff [14] has pointed out that this model gets into difficulty if the scaling is supposed to hold in qq scattering for finite virtual m_q because then the dominant scattering diagram is not fig. 3b, but the multiple wide angle scattering diagram fig. 4, (where none of the quarks is far from its mass shell), which gives

$$\frac{d\sigma}{dt}\,(\mathrm{pp}) \sim s^{-8} f(z). \tag{2.12}$$

Thus it is necessary either to suppress wide angle q-q scattering, and suppose that the q-q amplitude scales only for large m_q, or one must expect the behaviour (2.12) to supplant (2.11) at sufficiently large s (see also ref. [15]).

Halliday et al. [16] have criticized all the above models on the grounds that they assume dominance of two-particle exchange, and suggest that instead one might use the eikonal model to represent the sum of the leading order contributions to diagrams with arbitrary numbers of exchanges fig. 5, giving

$$\frac{d\sigma}{dt} \sim \frac{1}{s^2}\, e^{-a \log^2(s/b)}, \tag{2.13}$$

where a and b may be functions of z.

We are thus faced with the situation, which seems to be all too common in high-energy physics, that there exists a variety of proposed models, none of which can claim overwhelming theoretical plausibility, and all of which bear at

least some resemblance to the data. The difficulty of testing these models lies firstly in the uncertainty as to what constitutes asymptotia in s. Most comparisons have been made with $s < 50$ GeV^2 data which forces one to have a fairly small lower bound in s, and makes it hard to identify a large negative power of s with precision, though recently it has been possible to use the ISR pp data as well. The situation is further confused by the fact that possible log s dependences have been dropped from all the above equations. One might expect to get at least one power of log s for each loop integration in the amplitudes of figs. 1–4. Moreover, in an eikonal type of theory (2.13) [16] the power behaviours will themselves be modified by logarithmic corrections, say

$$n \to n + n_2 \log s. \tag{2.14}$$

Also of course with low-energy data the power of s obtained is considerably influenced by any assumptions which may be made about $f(z)$. It is clearly necessary therefore to try and use data over a wide range of s, one in which log s changes significantly, if we are really to test these models.

However, there is also a problem as to the minimum value of $|t|$ which should be used. (2.1) is incompatible with the small $|t|$ data as it stands, though various suggestions have been made for iterating it in s (eikonalization) [6, 17], or in t (to build up reggeons as q-$\bar{\text{q}}$ bound states) [18]. In any event, the large angle behaviour should match on to the Regge behaviour at small $|t|$, but the position of the boundary is unclear. In ref. [11] a fixed t boundary at $|t_B| = 2.5$ GeV^2 is preferred, while ref. [18] favours something between a fixed t and a fixed z boundary.

A related problem concerns the effective trajectory at large $|t|$ (i.e. the s dependence at fixed t rather than fixed z.) In some of the above models [2, 18] the trajectories are expected to asymptote to negative integers, so $\alpha_{pp}(-\infty) = -2$ for ref. [13] or -3 for ref. [9]. Ref. [19] finds that $\alpha_{pp} \to -2$ phenomenologically, while ref. [12] claims it continues to fall with t, $\alpha_{pp}(t) \to 1 + 0.43t$, but the difference depends on both the data selection, and the Regge parametrization used.

We shall examine some of these questions below.

3. The pp elastic scattering data

A problem encoutered in evaluating models for the fixed z behaviour of scattering processes is that most of the high-energy data is published at a selection of t values at fixed s, and so interpolation is needed to construct fixed angle data sets. For $s < 50$ GeV^2 $d\sigma/dt$ data is available over the whole angular range [20] ($z = 1 \to 0$) at various energies though it is rather sparse at the larger angles for high s (see fig. 6). But in the Serpukhov and NAL energy ranges so far only small angle, $|t| < 1.4$ GeV^2, data is available, which is no help to us. In the ISR range there is now data [21] for $|t| < 5.5$ GeV^2 corresponding to $1 > z > 0.996$, but at accelerator energies this z region corresponds to $|t| < 0.1$ where one would certainly not expect scaling to occur, so it is not possible to relate these two sets of high $|t|$ data directly.

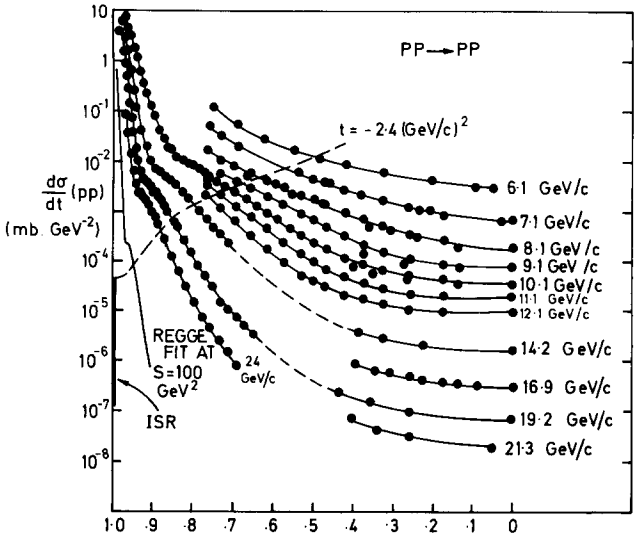

Fig. 6. $d\sigma/dt(pp)$ at various values of s plotted against z (from refs. [20, 21]). The boundary of the scaling region is shown at $|t| = 2.4$ GeV^2. Also shown is the prediction of the Regge fit of ref. [23] at $s = 100$ GeV^2.

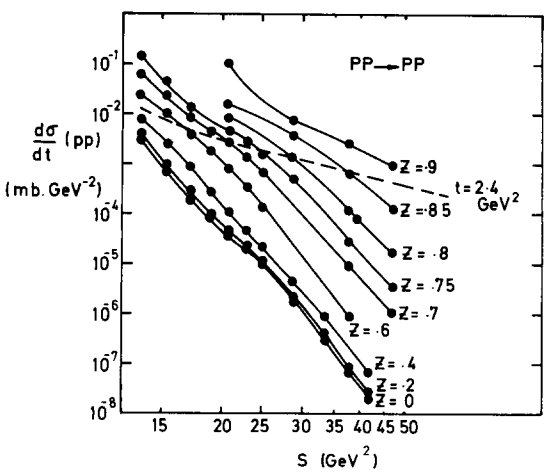

Fig. 7. Interpolated values of the pp data of fig. 6 plotted against s for chosen values of z. The boundary of the scaling region at $|t| = 2.4$ GeV^2 is shown.

However, we have recently published various Regge fits [22, 23] of pp and $\bar{p}p$ scattering data for $s > 15$ GeV^2, $|t| < 5.5$ GeV^2, which are in excellent quantitative agreement with the observed cross sections at both low and high energies, and which should, we feel, give a fairly reliable interpolation between them. The fits are based on a pomeron pole (P) with $\alpha_P(0) \approx 1.06$ to give the rise in σ_{tot},

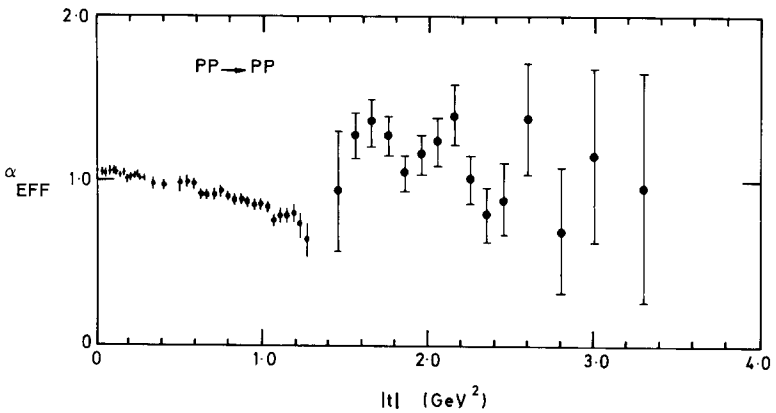

Fig. 8. The effective trajectory of the ISRPP data (from ref. [24]).

secondary P′ and ω trajectories, and a core term (c) to account for the high s, large $|t|$, data. (For definitness we have concentrated on fit (iii) of ref. [23], but the conclusions are similar for fit (ii) as well.) We have used the fit to provide an interpolation of the data for the range $50 < s < 3000$ GeV^2, $0 < |t| < 5.5$ GeV^2. When supplemented by an interpolation of the actual data for $13 < s < 50$ GeV^2 this enables us to span the whole range $0.998 \geqslant z \geqslant 0$ even though we restrict ourselves to a scaling region of $|t| > 2.4$ GeV^2 (see fig. 7).

In order to be able to quote a comparative χ^2 for our various fits to this interpolated "data" we have assigned 10% conventional errors over the whole range. This is clearly more realistic in some s and t regions than others, but it is used only to provide a yardstick by which to evaluate the different models. Our high-energy amplitudes have of course the phases of the Regge pole terms and are thus compatible with dispersion relations, but as we are fitting with models for $d\sigma/dt$ rather than the amplitudes themselves these phases are irrelevant. Scaling models do not predict the phases in general, though those which require real large $|t|$ amplitudes seem already to be ruled out by the dip in $d\sigma/dt$ (pp) at $|t| = 1.4$ GeV^2.

Before we discuss our fits in detail a qualitative feature of the large $|t|$ ISR data is worth noting, namely that for $|t| > 2.4$ $d\sigma/dt$ is approximately independent of s. This is illustrated in the effective trajectory plot (fig. 8 taken from ref. [23]) which shows that whereas the energy dependence of the low energy data is not incompatible with $\alpha(t) \underset{t \to \infty}{\to} -2$ as required by ref. [18], this is certainly not proven (see also ref. [19] and contrast ref. [12]); at high energies $\alpha_{\text{eff}} \approx 1$ within large errors, so there is no sign of the onset of this limiting behaviour.

This could be taken to indicate that the minimum $|t|$ value for scaling is higher at large s than at small s, as also suggested in ref. 18. On the other hand if we have, at fixed z, the behaviour (2.5), and $d\sigma/dt$ is independent of s, then at fixed s we must have

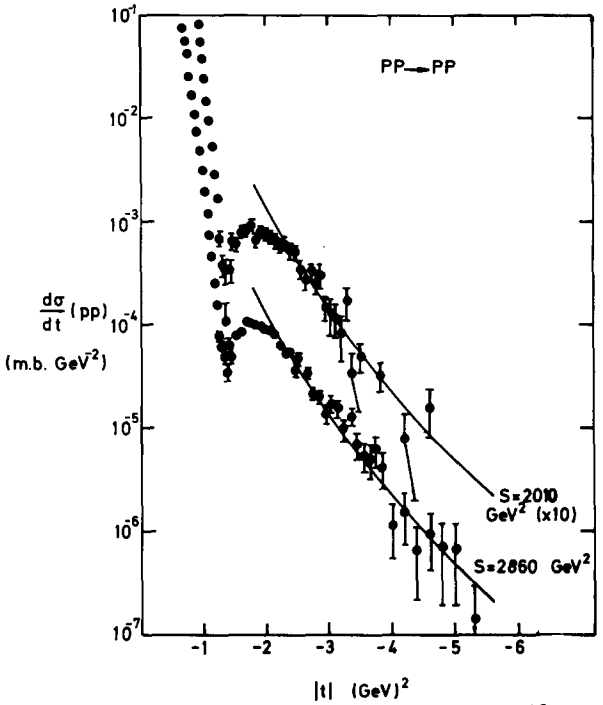

Fig. 9. The large $|t|$ (> 2.4 GeV^2) ISR data fitted with $(t-2.0)^{-10}$. Clearly the power of t is not well determined because of the small range of t available.

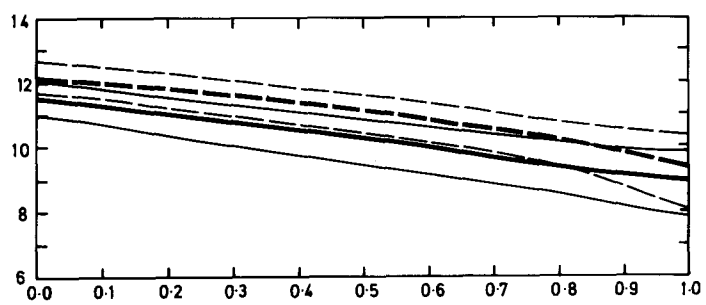

Fig. 10. $f(z)$ for $n = 8$, 10, 12. The solid lines are fits to the interpolated data of fig. 7. The dashed lines are fits to 'data' from fit (iii) of ref. [23].

$$\frac{d\sigma}{dt} \sim \frac{1}{(t_1 - t)^n} \,. \tag{3.1}$$

In fig. 9 we show the large $|t|$ ISR data compared with (3.1) for $n = 10$, and evidently the agreement is quite good (remembering that the energy independence

is only approximate) but other n values in the neighbourhood are equally satisfactory (see sect. 6).

Since, as we discussed in refs. [22–24], the logarithmic slope of $d\sigma/dt$ is much smaller in this region than one would expect (from for example simple Regge cut and other rescattering models which would lead us to expect half the logarithmic slope of the small $|t|$ data) it could be that this slope is determined by the onset of a scaling behaviour rather than multiple scattering effects [24]. This will be explored further below.

4. The s-dependence

The various models of scaling behaviour discussed in sect. 2 have led us to examine the following parameterizations for wide angle scattering:

The scaling law (refs. [7–13])

$$\frac{d\sigma}{dt} = \frac{1}{s^n} f(z). \tag{i}$$

Scaling with logarithmic corrections

$$\frac{d\sigma}{dt} = \frac{1}{s^n} (\log s)^{n_1} f(z). \tag{ii}$$

Logarithmic corrections to the power behaviour (ref. [16])

$$\frac{d\sigma}{dt} = \frac{1}{s^{n+n_2 \log s}} f(z). \tag{iii}$$

In fig. 10 we show the power of n obtained in fitting our interpolated "data" for $24 < s < 3000$ GeV^2, $|t| > 2.4$ GeV^2 (as described in sect. 3) at fixed values of z, with parameterization (i). Good fits are obtained at each z, and the value n decreases from 11.5 to about 9 as z (and hence the range of s fitted, see fig. 6) is increased. It is evident from fig. 7 that if we take a lower s cut off than 25 GeV^2 a single power will not suffice. This high cut off accounts for the different between these results and the conclusions of some other authors [7, 11, 12]. However, we have not included the data of ref. [25] at $s = 60$ which suggests that even higher values of n ($\simeq 11$–12) may occur for small z and $s > 50$ GeV^2 (see also refs. [8, 9]).

Also shown in fig. 10 is the effect of fitting the $s > 24$ GeV^2 data with parameterization (ii), n_1 being fixed at 2, as suggested by the single loop amplitude of fig. 2. The $\log^2 s$ makes it possible to fit over a somewhat larger s range in fact ($s > 13$ GeV^2) but does not affect the conclusions significantly except that n is uniformly increased, as would be expected. Similarly, we have found that taking $n_1 = 4$ (as suggested by fig. 1) increases n further, while $n_1 = -2$ decreases n_1. The fits improve, but not significantly, with increasing n_1.

We have also attempted to fit with (iii), but the amount of data and the range of s available at a given z is insufficient to determine the extra parameter n_2.

We conclude from these fits that the data is unable to distinguish between the different parameterizations (i)–(iii), since all three are able to fit satisfactorily. In each case there is a lower bound on $|t|$ of about 2.4 GeV^2 which is independent of the energy, with a rapid departure of the data from the scaling curve at smaller $|t|$ as one goes into the dip at $|t|$ 1.4 GeV^2. The lower bound in s is about 24 GeV^2 for a single power (i), but can be lower if log s terms are included. Most important however, it is clear from fig. 10 (and also apparent in fig. 7) that n tends to decrease as z increases, so the high energy data with z near 1 seems to require a lower power of s.

5. The z-dependence

Since n does not vary greatly (within the large errors) over the whole angular range it is interesting to test the effect of fixing it at the various values suggested by the models described in sect. 2, (i.e. $n = 8$, 10 and 12) and determine the corresponding $f(z)$.

In fig. 11 we plot $f(z)$ obtained from our interpolated "data" using (i) with these values of n. The plots show that (as noted in refs. [8, 9, 11]) the form

$$f(z) = \frac{a}{(1-z^2)^m}$$

works surprisingly well, though with different values of m in the ISR and accelerator regimes. Obviously, the goodness of fit varies somewhat with z, depending on how far the power of n which is used differs from the optimal value given in fig. 10. However, we also want to emphasize that there is a strong correlation between the values of m obtained and the chosen n. In fact they are approximately linearly related in both regimes. Our results thus contrive to be in approximate accord with the apparantly rather different conclusions of ref. [11], $n = 9.7$, $m = 7$ and of ref. [8], $n = 12$, $m = 6$. The effect of using parameterisation (ii) instead, with say $n_1 = 2$, is not significantly different from the above.

6. The angle dependence and form factors

The rather straightforward z dependence shown in fig. 11 implies that one may be able to fit all the data with simple parameterizations of $f(z)$. In so doing it is no longer necessary to interpolate the data to chosen z values, but we can fit the actual experimental data at both accelerator and ISR energies (the data of ref. [21], normalized as described in ref. [26]). Again, we restrict ourselves to $s >$ 24 GeV^2, $|t| > 2.4$ GeV^2.

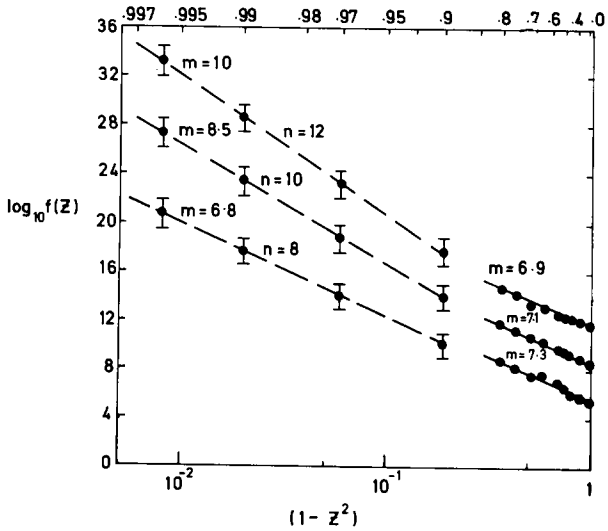

Fig. 11. $f(z)$ for n = 8, 10, 12. The solid lines are fits to the interpolated data of fig. 7. The dashed lines are fits to 'data' from fit (iii) of ref. [23].

Fig. 11 suggests that we try

$$f(z) = \frac{a}{(1-z^2)^m} . \qquad \text{(a)}$$

We have attempted to use (a) in parameterization (i) to fit all the data, and the resulting parameters are given in table 1. (In an obvious notation we call this fit (ia)). Not surprisingly, the χ^2 per point is poor because, as is evident from fig. 11, the accelerator and ISR regions prefer different values of m. The best values obtained in fits to these two regions separately are also given in table 1, and are in agreement with fig. 11. However, the n value of the ISR fit differs somewhat from fig. 10 because of the influence of $f(z)$.

The use of (a) in parameterization (ii) (fit(iia)) is very similar to the above but the χ^2 is somewhat worse. However, now that we have fixed on a form for $f(z)$ it is possible to use parameterization (iii) as well and determine n_2, because high and low s are fitted simultaneously. As the table shows the value of n is raised considerably, and the overall fit is much better. See fig. 12. We discuss a varient of this model below.

The obvious criticism which can be made of (a) is that $f(z) \to \infty$ as $z \to 1$ so there is bound to be some difficulty at small angles. It seems more realistic to move this singularity out of the physical region, and a simple way to do this is suggested by the model discussed in sect. 2, i.e. to use a form factor like

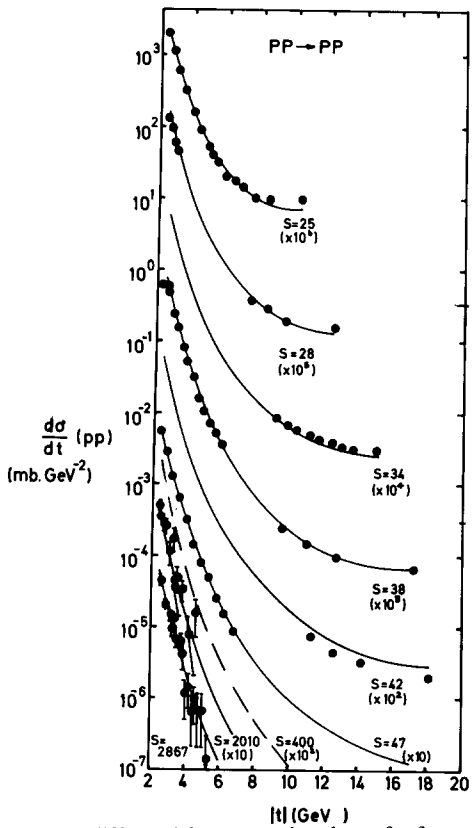

Fig. 12. A fit to the pp differential cross section data of references [20, 21] using parameterization iii(a) (solid lines). A prediction is given at $s = 400\ \mathrm{GeV}^2$ (dashed line).

$$G(t) = \frac{1}{(1-t/t_1)^{\frac{1}{2}m}} \quad , \tag{6.1}$$

(where physically for protons $t_1 \approx 0.71, m \approx 4$) and symmetrize by writing

$$\frac{\mathrm{d}\sigma}{\mathrm{d}t} = \frac{a}{s^l} \left[G(t)\, G(u)\right]^2 \quad , \tag{6.2}$$

which gives us parameterization (i) with

$$f(z) = a \left[\left(1 + \frac{2t_1}{s}\right)^2 - z^2 \right]^{-m} \quad , \tag{b}$$

$n = l + 2m.$

The fits (ib) reported in table 1 show the results of comparing this formula with all the data, and with high and low energies separately. The fit is an improvement over (ia) but again the two regions really prefer different values of the parameters. The values of n in the overall fit is close to that which would be obtained from the dipole with $l = 0$, but the value of m is much higher. Again the n value at ISR is rather low.

Correspondingly with parameterization (iib), $n_1 = 2$, we are able to fit as well, and the only difference is to lower n a bit.

With (iiib) the extra freedom provided by n_2 enables us to get a better description of the data, by adjusting to give the desired energy dependence at low energy, and the approximate energy independence of the ISR data, at fixed t. But the value of m is clearly quite different from that of the form factor, and t_1 is very small (see below).

However it is well known that the dipole form (6.1) is not a very good description of the proton's electromagnetic form factor at larger $|t|$, which is better represented by [27]

$$G(t) = \left[\left(1-\frac{t}{0.382}\right)\left(1-\frac{t}{2.10}\right)\left(1-\frac{t}{14.0}\right)\right]^{-1}, \tag{6.3}$$

though the asymptotic behaviour $\sim t^{-3}$ then contradicts the usual scaling assumptions [2]. If (6.3) is symmetrized like (6.1) we get

$$f(z) = a\left\{\left[\left(1+\frac{0.764}{s}\right)^2 - z^2\right]\left[\left(1+\frac{4.20}{s}\right)^2 - z^2\right]\left[\left(1+\frac{28.0}{s}\right)^2 - z^2\right]\right\}^{-2},$$

$$n = l + 12. \tag{c}$$

With this form we obtain the fits (ic) given in table 1. They have fewer free parameters than (ib), and are even less satisfactory overall, though the fit to ISR data alone, with its rather limited t range, is moderate. Similar remarks apply to (iic) and (iiic).

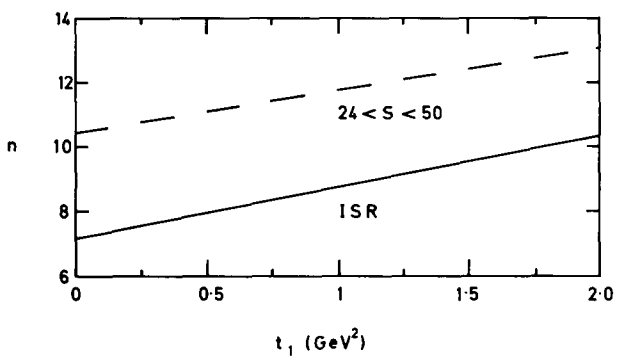

Fig. 13. n as function of t_1 using parameterization i(a) in the energy regions above.

Table 1

Model	s Range [a]	n	m	$\log_{10} a$	t_1	n_2	n_3	χ^2/Point M	I	A
	M	10.45	7.15	9.35				2.4		
i(a)	I	7.15	6.87	3.03					1.3	
	A	7.94	7.24	5.37				15.8	2.9	14.4
	M	11.48	8.24	11.20	0.71			2.2		
i(b)	I	8.50	8.40	5.61	0.85				1.2	
	A	9.08	8.40	7.46	0.83			14.0	1.9	12.5
	M	12.69		14.21				20.0		
i(c)	I	7.98		9.69					7.2	
	A	11.41		12.26				24.2	26.0	24.6
	M	11.51	7.22	9.87				2.7		
ii(a)	I	7.64	6.87	3.44					2.0	
	A	8.24	7.19	4.74				17.5	3.0	15.7
	M	11.33	7.60	9.70	0.61			2.3		
ii(b)	I	9.60	9.27	6.14	1.50				1.8	
	A	9.41	8.37	6.88	0.85			16.0	2.1	14.4
	M	11.96		12.03				21.8		
ii(c)	I	7.99		8.03					7.2	
	A	12.56		14.02				21.0	26.0	21.6
iii(a)	A	13.98	7.18	11.87		−0.53		3.3	1.3	3.1
iii(b)	A	13.95	7.22	11.87	0.02	−0.53		3.3	1.3	3.1
iii(c)	A	16.23		14.88		−0.86		34.3	9.7	31.5
iv(a)	A	10.66	5.28	9.68			0.52	2.5	2.9	2.5
iv(b)	A	11.10	6.48	10.56	0.63		0.45	2.5	2.6	2.5

[a] s Ranges: M($24 < s < 50$), I($950 < s < 3000$), A($24 < s < 3000$).

It is clear from table 1 that the n value required with parameterization (i) at low energies differs considerably from that needed to fit the ISR data, so it is not surprising that the attempt to fit the entire s range with a compromise set of parameters was unsatisfactory. This difference is illustrated further in fig. 13 where n is plotted against t_1 in fit (ib) for the two energy regions. (Of course, the χ^2/pt increases as one moves away from the best fit parameters of table 1): The energy independence of the ISR data at fixed t requires $n \simeq m$ and we find that similar values of m are also needed at low energies though n is quite different (see table 1). So n decreases with s but m is approximately independent of energy.

This accounts for the comparative success of model (iiib) which has different effective n's in the two regions (with n_2 negative). These fits have the rather strange feature that as s increases beyond the ISR regime the cross section is predicted to start increasing with s at fixed t, i.e. anti-shrinkage will set in in contrast to the shrinkage found at low energy. It is not inconceivable that this effect may actually be observed.

Since a and b in (2.13) can both be functions of z, more complicated parameterizations than (iii) are possible such as

$$\frac{d\sigma}{dt} = \frac{1}{s^{\bar{n}}} f(z),$$

$$\bar{n} \equiv n + n_3 \log(1-z^2) + n_2 \log s. \qquad \text{(iv)}$$

(Note that if $n_3 = n_2$ the power of s at fixed t becomes independent of $\log s$ for large s). The virtues of such a fit with $n = 4$, $n_3 = 0$, and $n_2 = 0.99$ are discussed in ref. [16]. The positive value of n_2 is due to the fact that these authors fit down to very low energies. We find a good fit with $n_2 = 0$ (see table 1). The effect of this parameterization is to increase the effective value of m with s while keeping n constant. This model also gives anti-shrinkage at large s.

7. Conclusions

Though these fits are necessarily somewhat inconclusive because the range of data available is too small the following points seem to stand out.

Firstly the larger $|t|$ ISR data, though approximately independent of s, have a t dependence which is not incompatible with the onset of scaling at $t \equiv t_B \simeq -2.4$ GeV^2 like at machine energies. This is in contrast with the expectation of a fixed z, or at least an s-dependent, boundary to the scaling region, obtained from some models (e.g. ref. [18]).

In ref. [11] it was suggested that the scaling behaviour might match smoothly onto the pomeron Regge pole behaviour at small t, leading to $t_B \approx -2.5$ GeV^2 if $\alpha_P(t) \approx 1 + 0.5t$. Our recent fits which give $\alpha_P(t) \approx 1.06 + 0.2t$ would suggest t_B in the region of 5 GeV^2 if one followed the same line of argument, but the presence of the dip in $d\sigma/dt$ at $|t| \approx 1.4$ GeV^2 makes it clear that the scaling region does not in fact run smoothly into the Regge behaviour. Rather, if the Regge pole and cut fits of ref. [24] are accepted, the scaling boundary corresponds to the onset of the dominance of $d\sigma/dt$ by the almost energy independent P $\otimes$ P cut. One might speculate that this cut is related to those found by Lovelace [28] in renormalizable field theories with Bjorken scaling. Certainly it is clear from fig. 8 that α_{eff} is not approaching a negative integer in the ISR region as required by ref. [18] (though it could be at low energies).

Though the errors are rather large we have found that the power behaviour in s decreases with increasing s from about $n \approx 11.5$ for $z \approx 0$ at machine energies, to $n \approx 9$ for small angles at ISR. (This situation is somewhat confused by the fact that the data of ref. [25] suggest that n is increasing with s at large angles for $s > 50$ GeV^2.) The interchange model with $n = 12$ or 10, depending on the version adopted, thus seems to be failing at high energy at it could be that the Landshoff diagram, fig. 4 [14], or eikonalization [16] is beginning to take over in the ISR

region. But more data at large $|t|$ are needed to check this conclusion properly because of the interpolations which we have been forced to make in using the ISR data. The addition of logarithmic factors in the parameterizations (ii) and (iii) has not made a great deal of difference, though the extra parameter in (iii) does enable one to get somewhat better simultaneous fits to the ISR and machine energy data.

The angular dependence, though rather simple both at machine energies (as noted by refs. [8, 9, 11] and at ISR, is somewhat different in the two cases, as fig. 11 shows, and though various parameterizations motivated by the behaviour of the electromagnetic form factor can fit either regime satisfactorily it is much harder to fit both together.

This could have several explanations. Perhaps $s < 50$ GeV^2 is too low and we are not really seeing scaling in the accelerator data (though all the other tests [2, 3] have perforce been made in this region). Or the apparent scaling at ISR may be an accident, and really $z \ll 0.98$ is necessary for a true scaling behaviour. Or it may simply be that a more complicated $f(z)$ than (a) (b) or (c), unrelated to the electromagnetic form factors, is required. Alternatively, our results may serve to reinforce the conclusion that scaling is really a rather low-energy phenomenon, and non-scaling terms such as fig. 4, or eikonalization corrections may break the scaling behaviour at large s. Similar conclusions are being drawn about scaling breakdown in deep inelastic scattering [29]. Large angle data at high energies is eagerly awaited to help in unravelling these problems.

References

[1] F.J. Gilman, Phys. Reports 4 (1972) 95.
[2] S.J. Brodsky, High energy collisions – 1973, ed. C. Quigg (AIP, New York, 1973); R. Blankenbecler and S.J. Brodsky, SLAC-PUB-1430 (1974), unpublished.
[3] P.V. Landshoff, Report to 17th Int. Conf. on high energy physics, London, July 1974.
[4] H.D.I. Abarbanel, S.D. Drell and F. J. Gilman, Phys. Rev. Letters 20 (1968) 280; Phys. Rev. 177 (1969) 2458.
[5] T.T. Wu and C.N. Yang, Phys. Rev. 137 (1965) B708.
[6] T.T. Chou and C.N. Yang, Phys. Rev. 170 (1968); 175 (1968) 1832.
[7] D. Horn and M. Moshe, Nucl. Phys. B48 (1972) 557.
[8] J.F. Gunion, S.J. Brodsky and R. Blankenbecler, Phys. Letters 39B (1972) 649.
[9] J.F. Gunion, S.J. Brodsky and R. Blankenbecler, Phys. Rev. D8 (1973) 287.
[10] P.V. Landshoff and J.C. Polkinghorne, Phys. Rev. D8 (1973) 927.
[11] P.V. Landshoff and J.C. Polkinghorne, Phys. Letters 44B (1973) 1.
[12] V. Barger, F. Halzen and J. Luthe, Phys. Letters 42B (1972) 428.
[13] S.J. Brodsky and G.R. Farrar, Phys. Rev. Letters 18 (1973) 1153.
[14] P.V. Landshoff, Cambridge University report DAMTP 73/36 (1973), unpublished.
[15] J.C. Polkinghorne, Phys. Letters B49 (1974) 277.
[16] I.G. Halliday, J. Huskins and C.T. Sachrajda, Phys. Letters 47B (1973) 509; Imperial College report ICTP/73/36 (1974), unpublished.
[17] M. Kac, Nucl. Phys. B62 (1973) 402.
[18] R. Blankenbecler, S.J. Brodsky, J.F. Gunion and R. Savit, Phys. Rev. D8 (1973) 4117.

[19] J.F. Gunion, Proc. of the 4th Int. Symp. on multiparticle hadrodynamics, Pavia, 1973.
[20] J.V. Allaby et al., Phys. Letters 25B (1967) 156; 28B (1968) 67; Nucl. Phys. B52 (1973) 316;
C.M. Ankenbrandt et al., Phys. Rev. 170 (1968) 1223;
C.W. Akerlof et al., Phys. Rev. 159 (1967) 1138.
[21] A. Bohm et al., Phys. Letters 49B (1974) 1.
[22] P.D.B. Collins, F.D. Gault and A. Martin, Phys. Letters 47B (1973) 171.
[23] P.D.B. Collins, F.D. Gault and A. Martin, Nucl. Phys. B80 (1974)135.
[24] P.D.B. Collins, F.D. Gault and A. Martin, Nucl. Phys. B83 (1975) 241.
[25] G. Cocconi et al., Phys. Rev. 138 (1965) 165.
[26] A. Martin, Nucl. Phys. B77 (1974) 226.
[27] N. Byers, Proc. of the 11th Int. School of subnuclear physics, Erice, Sicily, 1973.
[28] C. Lovelace, Rutgers University report (1974), unpublished.
[29] F. Gilman, Report to 17th Int. Conf. on high energy physics, London, July 1974.